.

Surface and size effects on phase diagrams of ferroelectric nanocylinders

Yue Zheng, S. P. Lin, and Biao Wang

Citation: Appl. Phys. Lett. **99**, 062904 (2011); doi: 10.1063/1.3624829
View online: http://dx.doi.org/10.1063/1.3624829
View Table of Contents: http://aip.scitation.org/toc/apl/99/6
Published by the American Institute of Physics

Surface and size effects on phase diagrams of ferroelectric nanocylinders

Yue Zheng,[a)] S. P. Lin, and Biao Wang[b)]
State Key Laboratory of Optoelectronic Materials and Technologies/Institute of Optoelectronic and Functional Composite Materials, School of Physics and Engineering, Sun Yat-sen University, Guang Zhou 510275, China

(Received 21 April 2011; accepted 8 July 2011; published online 11 August 2011)

Size-temperature phase diagrams of ferroelectric nanocylinder have been investigated. Taking into account existence of the depolarization field, surface and size effects, an eighth-order polynomial of the modified thermodynamic model has been established. Our results show that the phase diagrams obviously vary with ratio of the length and radius, and can be adjusted by the mechanical loads especially. © *2011 American Institute of Physics*. [doi:10.1063/1.3624829]

Properties of ferroelectric nanocylinder (FNC), taking various forms such as ferroelectric nanodisk (FND), nanorod (FNR) and nanowire (FNW), have been extensively studied due to a rapid surge of interest from nano-technology. Results show that ferroelectricity of FNC can be determined by its dimensions and other factors.[1–10] For example, simulations based on a first-principle have found that ferroelectricity of FNW disappears completely when the radius is below a critical value.[7] Morozovska *et al.*[8] indicated the surface tension effect significantly change properties of FNC. Based on stability analysis, analytic expressions of FNW with the surface tension effect have been derived by Zheng *et al.*[6,9] Meanwhile, their first principle calculations[10] have also confirmed that the enhanced polarization in FNW. Moreover, it is well-known that Pertsev *et al.*[11] studied the "misfit strain-temperature" (MST) phase diagrams of the ferroelectric thin film. Morozovska *et al.*[12] gave analytical expressions for the MST phase diagrams. Chen *et al.*[13] and Ma *et al.*[14] developed the phase field model to predict the MST phase diagrams. More importantly, Lin *et al.*[15] recently calculated the "size-temperature" (S-T) phase diagram of FNW.

In this paper, an eighth-order polynomial of FNC has been established. Considering the combined effects of the surface, surface tension, stress loads and depolarization field due to the imperfect screening in the electrodes, the S-T phase diagrams of FNCs, including FND, FNR and FNW, were investigated as functions of length, radius and external stress loads, respectively.

We consider the thermodynamic reference as a crystal of infinite extent (surfaceless) absent an applied field. Let $\mathbf{P}$ be the spontaneous polarization field, which is the polarization from the permanent electric moment formed from spontaneous atomic displacements generated in a dielectric when going through a ferroelectric phase transformation. $\mathbf{P^E}$ is the result of mechanisms such as the electronic polarization, and other non-permanent displacement of the ionic charge distribution. Therefore, the electric displacement field $\mathbf{D}$ can be expressed in terms of the linear-part $\mathbf{P^E}$ and non-linear-part $\mathbf{P}$ as[15–20]

$$\mathbf{D} = \varepsilon_0\mathbf{E} + \mathbf{P^E} + \mathbf{P} = \varepsilon_0\mathbf{E} + \chi_\mathbf{b}\mathbf{E} + \mathbf{P} = \varepsilon_\mathbf{b}\mathbf{E} + \mathbf{P}, \tag{1}$$

where $\chi_\mathbf{b}$ and $\varepsilon_\mathbf{b}$ are the background susceptibilities and dielectric constants, respectively. Since the background material is the paraelectric phase of cubic crystal symmetry, ε_b in three axis directions are the same, *i.e.*, $\varepsilon_{11b} = \varepsilon_{22b} = \varepsilon_{33b} = \varepsilon_b$.

The spontaneous polarization vector, $\mathbf{P} = (P_1, P_2, P_3)$, is usually used as the order parameter of the Landau-type free energy. Recently, an eighth-order P_i^8 polynomial of Landau-type potential has been employed for $BaTiO_3$ (BTO) material. In this regard, the free energy with considering effect of the mechanical stresses can be given by,[13,15,19]

$$\begin{aligned}\Delta G =\ & \alpha_1\left(P_1^2+P_2^2+P_3^2\right)+\alpha_{11}\left(P_1^4+P_2^4+P_3^4\right)\\ &+\alpha_{12}\left(P_1^2P_2^2+P_2^2P_3^2+P_3^2P_1^2\right)+\alpha_{111}\left(P_1^6+P_2^6+P_3^6\right)\\ &+\alpha_{112}\left[P_1^2\left(P_2^4+P_3^4\right)+P_2^2\left(P_1^4+P_3^4\right)+P_3^2\left(P_1^4+P_2^4\right)\right]\\ &+\alpha_{123}P_1^2P_2^2P_3^2+\alpha_{1111}\left(P_1^8+P_2^8+P_3^8\right)\\ &+\alpha_{1112}\left[P_1^6\left(P_2^2+P_3^2\right)+P_2^6\left(P_1^2+P_3^2\right)+P_3^6\left(P_1^2+P_2^2\right)\right]\\ &+\alpha_{1122}\left(P_1^4P_2^4+P_2^4P_3^4+P_3^4P_1^4\right)\\ &+\alpha_{1123}\left(P_1^4P_2^2P_3^2+P_2^4P_1^2P_3^2+P_3^4P_1^2P_2^2\right)\\ &-\tfrac{1}{2}s_{11}\left(\sigma_1^2+\sigma_2^2+\sigma_3^2\right)-s_{12}\left(\sigma_1\sigma_2+\sigma_2\sigma_3+\sigma_1\sigma_3\right)\\ &-\tfrac{1}{2}s_{44}\left(\sigma_4^2+\sigma_5^2+\sigma_6^2\right)-Q_{11}\left(\sigma_1P_1^2+\sigma_2P_2^2+\sigma_3P_3^2\right)\\ &-Q_{12}\left[\sigma_1\left(P_2^2+P_3^2\right)+\sigma_2\left(P_1^2+P_3^2\right)+\sigma_3\left(P_1^2+P_2^2\right)\right]\\ &-Q_{44}\left(P_2P_3\sigma_4+P_1P_3\sigma_5+P_2P_1\sigma_6\right),\end{aligned} \tag{2}$$

where α_i, α_{ij}, α_{ijk}, and α_{ijkl} are the dielectric stiffness coefficients. σ_i are the stress components. s_{ij} are the elastic compliance coefficients. Q_{ij} are the electrostrictive coefficients.

As shown in Fig. 1, we consider FNC with length h and radius R sandwiched between electrodes with the short-circuitboundary conditions. Generally speaking, ratio of length and radius for a FNW is very large. In order to facilitate discussion and compare with results of previous work,[4,15] we classify the FNC, according to $h < 0.5R$ (FND), $0.5R \le h < 4R$ (FNR), and $h > 4R$ (FNW), respectively. Under the absence of external electric field, the thermodynamic energy of a FNC should contain the contributions of the gradient, interface, surface, and depolarization field energies.[4–15] The gradient energy density is given by $\Delta G_{grad} = 1/2D_{ij}P_{i,j}P_{i,j}$, where D_{ij} are the gradient coefficients and $\partial P_i/\partial x_j$ are expressed by $P_{i,j}$.[13,15] The top and bottom interface energy and sidewall surface energy approximately acquire the forms as $G_\mathrm{I} = \int_0^R 2\pi r dr$ $\left[\frac{D_{11}}{\delta_\mathrm{I}}\left(P_1^2\big|_{z=\frac{h}{2}} + P_1^2\big|_{z=-\frac{h}{2}}\right) + \frac{D_{22}}{\delta_\mathrm{I}}\left(P_2^2\big|_{z=\frac{h}{2}} + P_2^2\big|_{z=-\frac{h}{2}}\right) + \frac{D_{33}}{\delta_\mathrm{I}}\right.$

[a)]Electronic mail: zhengy35@mail.sysu.edu.cn.
[b)]Electronic mail: wangbiao@mail.sysu.edu.cn.

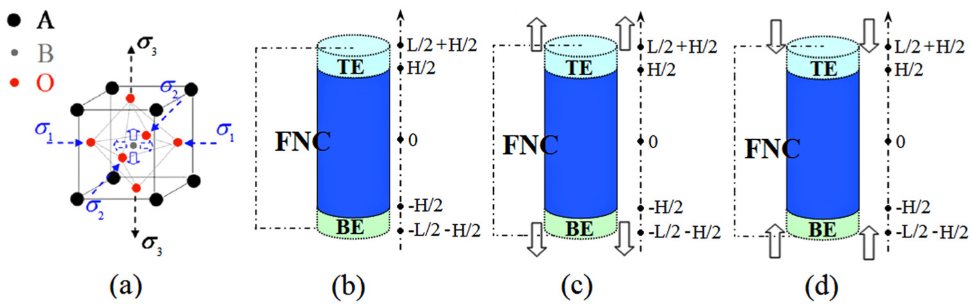

FIG. 1. (Color online) Schematic illustration of (a) the ABO_3 unit cell with compressive stresses along x and y directions and tensile stresses along z direction and (b) FNC with the top and bottom electrodes and external applied stresses.

$\left(P_3^2\big|_{z=\frac{h}{2}} + P_3^2\big|_{z=-\frac{h}{2}}\right)\Big]$ and $G_{\mathrm{s-w}} = 2\pi R\int_{-h/2}^{h/2}\left[\frac{D_{11}}{\delta_{\mathrm{s-w}}}P_1^2\big|_{r=R,z} + \frac{D_{22}}{\delta_{\mathrm{s-w}}}P_2^2\big|_{r=R,z} + \frac{D_{33}}{\delta_{\mathrm{s-w}}}P_3^2\big|_{r=R,z}\right]dz$, respectively, δ_{I} and $\delta_{\mathrm{s-w}}$ are the so-called extrapolation length for top and bottom interfaces and sidewall surface.

The depolarization energy of FNC is determined by the depolarization fields $\mathbf{E_d} = (E_{d1}, E_{d2}, E_{d3})$. Due to the imperfect screening in electrodes, the depolarization field E_{d3} in FNC can be given by $E_{d3} \approx -\eta(P_3 + q_e)/\varepsilon_b$, where η is estimated using the relation $\eta \approx 1/[1 + (\frac{h}{2R})^2]$ (Refs. 4 and 8) and q_e is the compensation charge density in the electrodes, approximately given by $q_e = -h\varepsilon_b(2l_s/\varepsilon_e + h/\varepsilon_b)^{-1}P_3$.[20] According to recent works about FNW,[15–19] it was known that appearance of P_1 and P_2 polarization components also induce the x-y depolarization fields E_{d1} and E_{d2}. In fact, the stable x-y plane polarization components exhibit a quasi-axisymmetric radial distribution in the x-y plane in FNW from the molecular dynamic and first principle simulation, and the total polarizations in the x-y plane are zero.[15] In this regard, the effective influence of the x-y plane depolarization fields can be approximately neglected.

Following Landau *et al.*,[21] for a non-zero electric field in the ferroelectrics, the thermodynamic potential should be obtained by starting from the relation as $d\Phi/d\mathbf{E} = -\mathbf{D}$. In this case, the fact that the spontaneous polarization $\mathbf{P}$ has no explicit functional dependence on $\mathbf{E}$, the thermodynamic potential of ferroelectrics based on Landau and Lifshitz (LL) theory can be given by $\Phi = \Phi|_{\mathbf{E}=0} - \mathbf{P}\cdot\mathbf{E} - \int_0^E \varepsilon_{\mathbf{b}}\cdot\mathbf{E}d\mathbf{E}$.[16] In addition, based on the discussions about the renormalized coefficients of the Landau-type Gibbs free energy and LL free-energy functional with an eighth-order polynomial,[13,19,22] we employed a modified thermodynamic potential of FNC taking into account effects of the depolarization field, interface, surface, and surface tension and on which polynomial can be written as

$$
\begin{aligned}
\Delta G^* = {} & \alpha_1^*(P_1^2+P_2^2) + \alpha_3^* P_3^2 + \alpha_{11}(P_1^4+P_2^4+P_3^4) \\
& + \alpha_{12}(P_1^2P_2^2+P_2^2P_3^2+P_3^2P_1^2) + \alpha_{111}(P_1^6+P_2^6+P_3^6) \\
& + \alpha_{112}\left[P_1^2(P_2^4+P_3^4)+P_2^2(P_1^4+P_3^4)+P_3^2(P_1^4+P_2^4)\right] \\
& + \alpha_{123}P_1^2P_2^2P_3^2 + \alpha_{1111}(P_1^8+P_2^8+P_3^8) \\
& + \alpha_{1112}\left[P_1^6(P_2^2+P_3^2)+P_2^6(P_1^2+P_3^2)+P_3^6(P_1^2+P_2^2)\right] \\
& + \alpha_{1122}(P_1^4P_2^4+P_2^4P_3^4+P_3^4P_1^4) \\
& + \alpha_{1123}(P_1^4P_2^2P_3^2+P_2^4P_1^2P_3^2+P_3^4P_1^2P_2^2) \\
& - (s_{11}+s_{12})\sigma_s^2 - \tfrac{1}{2}s_{11}\sigma_z^2 - 2s_{12}\sigma_s\sigma_z - P_3E_d - \tfrac{1}{2}\varepsilon_b E_d^2,
\end{aligned}
\tag{3}
$$

where the normalized coefficients α_1^* and α_3^* are the functions of size and stress and can be approximately given by $\alpha_1^* = \alpha_0(T-T_{c0}) + \frac{(Q_{11}+Q_{12})\mu}{R} - Q_{12}\sigma_z + \frac{K_1^R}{R^2} + \frac{K_1^h}{h^2}$, $\alpha_3^* = \alpha_0(T-T_{c0}) + \frac{2Q_{12}\mu}{R} - Q_{11}\sigma_z + \frac{K_2^R}{R^2} + \frac{K_2^h}{h^2}$.[15,22] σ_s is the uniform compressive radial stress induce by the surface tension, given by $\sigma_s = -\mu/R$, where μ is the effective surface tension coefficient. σ_z is the external applying stress along z direction. Based on the discussions about the renormalized coefficients of the Landau-type free energy on ferroelectrics in nanoscale,[8,15,22] coefficients of K_1^R, K_2^R, and K_1^h, K_2^h can approximately be expressed as functions of the dielectric stiffness coefficient α_0, so-called extrapolation length $\delta, \delta_{\mathrm{I}}$ and gradient-coefficients-dependent parameter $\zeta, \zeta_{\mathrm{I}}$, i.e., $K_1^R \approx K_2^R = \zeta\delta/\alpha_0$ and $K_1^h \approx K_2^h = \zeta_{\mathrm{I}}\delta_{\mathrm{I}}/\alpha_0$.

In following calculations, the S-T phase diagrams of FNC sandwiched between Pt electrodes are investigated. Electrostrictive and elastic coefficients,[13,19] background dielectric constant,[16] coefficients of electrode,[4] surface tension and surface effect[8,15,22] are well-known. According to possible phases,[11,15] the following notation for the different equilibrium phases may occur in FNC: (i) the p phase, where $P_1 = P_2 = P_3 = 0$; (ii) the c phase, where $P_3 \neq 0$ and $P_1 = P_2 = 0$; (iii) the aa phase, where $P_1 = P_2 \neq 0$ and $P_3 = 0$; and (iv) the r phase, where $P_1 = P_2 \neq 0$ and $P_3 \neq 0$. We only investigate the phase transitions with temperature cooling-down due to the first order phase transition of BTO FNC from the paraelectric state to ferroelectric state. The phase transition temperature of FNC is defined as $T_c = \max[T_{c1,2}, T_{c3}]$, here $T_{c1,2}$ and T_{c3} are the phase transition temperatures of the paraelectric phase losing its stability with respect to the appearance of P_1, P_2 and P_3, respectively, and can be obtained by setting $\alpha_1^* = 0$ and $\alpha_3^* = 0$,[7,11]

$$
\begin{aligned}
T_{c1,2} &= T_{c0} - \frac{Q_{11}+Q_{12}}{\alpha_0}\frac{\mu}{R} + \frac{Q_{12}}{\alpha_0}\sigma_z - \frac{K_1^R}{\alpha_0 R^2} - \frac{K_1^h}{\alpha_0 h^2}, \\
T_{c3} &= T_{c0} - \frac{2Q_{12}}{\alpha_0}\frac{\mu}{R} + \frac{Q_{11}}{\alpha_0}\sigma_z - \frac{K_2^R}{\alpha_0 R^2} - \frac{K_2^h}{\alpha_0 h^2},
\end{aligned}
\tag{4}
$$

In addition, minimizing the free energy function with respect to the polarization component P_i, *e.g.*, $\partial\Delta G^*/\partial P_i = 0$, the equilibrium values of P_i can be solved as function of temperature, length, radius and applied stresses.[12–16]

In our results, the normalized temperature $T/T_{\mathrm{C}}^{\mathrm{bulk}}$ will be given as function of radius and length, $T_{\mathrm{C}}^{\mathrm{bulk}}$ is the phase transition temperature of the bulk material.[11] Fig. 2(a)–2(c) show the S-T diagrams of the free standing BTO FNCs with lengths of 10 nm, 15 nm and 80 nm, respectively. It can be seen that T_{c3} is always higher than $T_{c1,2}$ because the surface

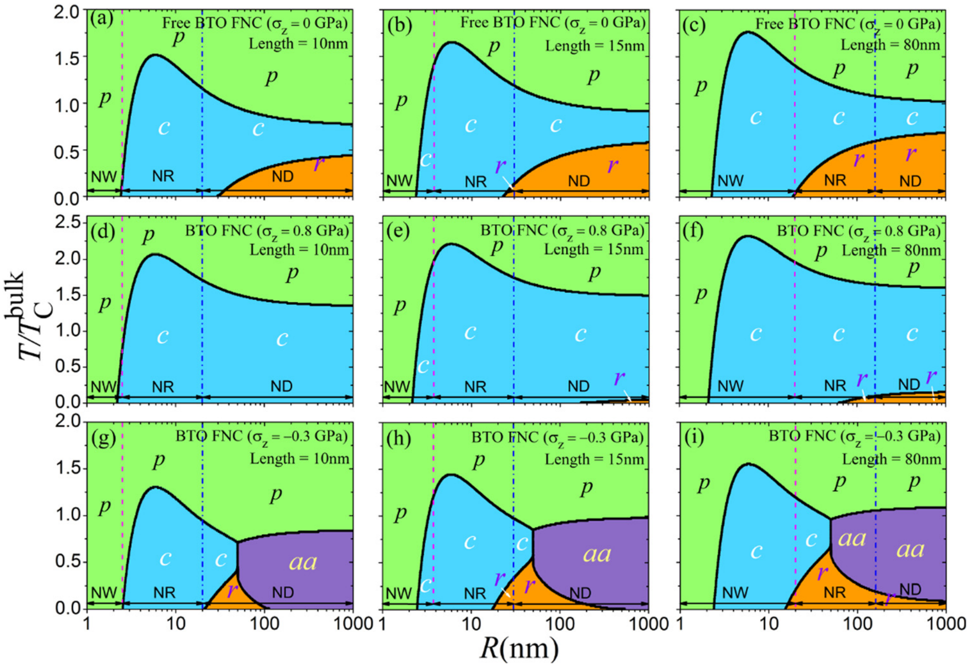

FIG. 2. (Color online) The S-T phase diagrams of BTO FNCs without external stress load at the lengths of (a) 10 nm, (b) 15 nm, and (c) 80 nm; with tensile stress load, $\sigma_z = 0.8$ GPa, at the lengths of (d) 10 nm, (e) 15 nm, and (f) 80 nm; and compressive stress load, $\sigma_z = -0.3$ GPa, at the lengths of (g) 10 nm, (h) 15 nm, and (i) 80 nm.

tension always enhances the polarization P_3 and on the contrary decreases the polarization P_1 and P_2. With the short circuit boundary conditions, size effect of FNC determined by the depolarization field and extrapolation length should be considered. Fig. 2(a)–2(c) also show that co-effects of the surface tension and size effects result in the peak of T_{c3}. Size effect induces appearance of the critical radius $R_c \approx 2.4$nm, below which ferroelectricity of FNC disappear. Moreover, results in Fig. 2(a)–2(c) indicate that the *r*-phase magnifies and c-phase shrinks with the length increasing. When the radius is large enough, the phase transition temperature is close to T_C^{bulk} because both of the surface tension and size effects are very weak.

The S-T phase diagrams of the FNCs controlled by the external stress load σ_z were also developed. Fig. 2(d)–2(f) show the S-T phase diagrams of FNC with a applied tensile stress of $\sigma_z = 0.8$ GPa. It can be seen that the tensile stress results in the *c*-phase to dominate and the *r*-phase to shrink or even to be vanished. It is known the compressive stress can reduce the polarization P_3 and enhance P_1 and P_2 of FNC,[12,15] and also adjust the S-T phase diagram. Results of Fig. 2(g)–2(i) show that the compressive stress, *i.e.*, $\sigma_z = -0.3$ GPa, induces the appearance of the *aa*-phase and shifts the *c*-phase and the *r*-phase as whole to shrink.

In summary, a modified thermodynamic model to investigate effects of the surface tension, depolarization field and external mechanical load on the S-T phase diagrams of FNC with the short circuit boundary conditions is established. Our results show that the phase transition temperature of FNC is determined by its radius and lengths due to the surface tension, surface and depolarization field effects. More importantly, the S-T phase diagrams of FNCs can be controlled by radius and lengths of FNCs, and controlled by the applied stresses.

This project was supported by the NSFC (Nos. 10902128, 10732100, 11072271, 10972239), and the Fundamental Research Funds for the Central Universities.

[1]J. F. Scott, Science **315**, 954 (2007).
[2]I. I. Naumov, L. Bellaiche, and H. X. Fu, Nature **432**, 737 (2004).
[3]L. Louis and P. Gemeiner *et al.*, Nano Lett. **10**, 1177 (2010).
[4]Y. Zheng and C. H. Woo, J. Appl. Phys. **107**, 104120 (2010).
[5]A. N. Morozovska *et al.*, J. Appl. Phys. **108**, 042009 (2010).
[6]Y. Zheng, C. H. Woo, and B. Wang, Nano Lett. **8**, 3131 (2008).
[7]I. I. Naumov and H. X. Fu, Phys. Rev. Lett. **95**, 247602 (2005).
[8]A. N. Morozovska *et al.*, Phys. Rev. B **73**, 214106 (2006).
[9]Y. Zheng *et al.*, J. Phys.: Condens. Matter. **20**, 125216 (2008).
[10]M. Q. Cai, Y. Zheng *et al.*, Appl. Phys. Lett. **95**, 232901 (2009).
[11]N. A. Pertsev *et al.*, Phys. Rev. Lett. **80**, 1988 (1998).
[12]M. D. Glinchuk *et al.*, J. Appl. Phys. **99**, 114102 (2006).
[13]Y. L. Li and L. Q. Chen, J. Appl. Phys. **98**, 064101 (2005).
[14]D. C. Ma, Y. Zheng *et al.*, Appl. Phys. Lett. **95**, 262901 (2009).
[15]S. P. Lin, Y. Zheng *et al.*, Appl. Phys. Lett. **96**, 232904 (2010).
[16]Y. Zheng and C. H. Woo, Appl. Phys. A **97**, 617 (2009); C. H. Woo and Y. Zheng, Appl. Phys. A **91**, 59 (2008).
[17]A. K. Tagantsev, Ferroelectrics **375**, 19 (2008).
[18]M. E. Lines and A. M. Glass, *Principles and Applications of Ferroelectrics and Related Materials* (Clarendon, Oxford, 1979).
[19]Y. L. Li and L. Q. Chen, Appl. Phys. Lett. **88**, 072905 (2005).
[20]R. R. Mehta *et al.*, J. Appl. Phys. **44**, 3379 (1973).
[21]L. D. Landau, E. M. Lifshitz, and L. P. Pitaevskii, *Electrodynamics of Continuous Media* (Oxford University Press, London, 1984).
[22]S. Lin *et al.*, Phys. Rev. B **74**, 134115 (2006).